Quantum phase detection generalisation from marginal quantum neural network models

Preprint · August 2022

CITATIONS
0

READS
38

5 authors, including:

Saverio Monaco
University of Padova
1 PUBLICATION **0** CITATIONS
SEE PROFILE

Oriel Kiss
University of Geneva
7 PUBLICATIONS **4** CITATIONS
SEE PROFILE

Antonio Mandarino
University of Gdansk
32 PUBLICATIONS **292** CITATIONS
SEE PROFILE

Michele Grossi
CERN
32 PUBLICATIONS **240** CITATIONS
SEE PROFILE

Quantum phase detection generalisation from marginal quantum neural network models

Saverio Monaco,[1,2] Oriel Kiss,[1,3,*] Antonio Mandarino,[4] Sofia Vallecorsa,[1] and Michele Grossi[1,†]

[1] *European Organization for Nuclear Research (CERN), Geneva 1211, Switzerland*
[2] *Department of Physics, University of Padova, 35122 Padova PD, Italy*
[3] *Department of Particle and Nuclear Physics, University of Geneva, Geneva 1211, Switzerland*
[4] *International Centre for Theory of Quantum Technologies, University of Gdańsk, Wita Stwosza 63, 80-308 Gdańsk, Poland*

(Dated: August 19, 2022)

Quantum machine learning offers a promising advantage in extracting information about quantum states, e.g. phase diagram. However, access to training labels is a major bottleneck for any supervised approach, preventing extracting insights about new physics. In this work, using quantum convolutional neural networks we overcome this limit with the determination of the phase diagram of a model where no analytical solutions are known, by training on marginal points of the phase diagram where integrable models are represented. More specifically, we consider the Axial Next Nearest Neighbor Ising (ANNNI) Hamiltonian, which possesses a ferro-, para-magnetic and antiphase and we show that the whole phase diagram can be reproduced.

Introduction: Quantum machine learning (QML) [1], where parametrized quantum circuits [2] act as statistical models, has attract much attention recently, with applications in the natural sciences [3–8] or in generative modeling [9–13]. Even if QML models benefit from high expressivity [14] and demonstrated superiority over classical models in some specific cases [15, 16], it is still unclear what kind of advantage could be obtained with quantum computers [17] in the era of foundation models [18].

Quantum data, on the other hand, could be a natural paradigm to apply QML, where quantum advantages have already been demonstrated [19]. There is hope that quantum data could be collected via quantum sensors [20], and eventually linked to quantum computers. In this work, we emulate the possibility of working with quantum data by constructing them directly on a quantum device. Specifically, this letter addresses the computation of the phase diagram of a Hamiltonian H using a supervised learning approach. Even if similar problems have already been explored for the binary case [21, 22], with multiples classes [23] and computed on a superconducting platform [24], all of these approaches suffer from a limitation by construction, a bottleneck. In fact, since labels are needed for the training, and because they are computed analytically or numerically, these techniques can only speed up calculations, but cannot extend beyond their validated domain. Alternatively, Kottmann *et al.* [25] proposed to use anomaly detection (AD), an unsupervised learning technique, as a way to bypass the bottleneck of having classical training labels, by finding structure inside the data set.

This letter numerically demonstrates that supervised QML can make predictions to regions where analytical labels do not exist, after being only trained on easily computable sub-regions. Moreover, QML only needs very few training labels to do so, as already pointed out by Caro *et al.* [26]. This drastically changes the perspective, extending QML capabilities to extrapolate and eventually discover new physics when trained on well-established simpler models.

The model: We consider the Axial Next Nearest Neighbour Ising (ANNNI) model

$$H = J\sum_{i=1}^{N}\sigma_x^i\sigma_x^{i+1} - \kappa\sigma_x^i\sigma_x^{i+2} + h\sigma_z^i, \tag{1}$$

where σ_a^i are the Pauli matrices acting on the $i-$th spin, $a = \{x, y, z\}$, and we assume open boundary conditions. The energy scale of the Hamiltonian is given by the coupling constant J (without loss of generality we set $J = 1$), while the dimensionless parameters κ and h account for the next-nearest-neighbor interaction and the transverse magnetic field, respectively. We restrict ourselves to $\kappa \geq 0$, $h \geq 0$ and even N. The difference of sign between the nearest and next-nearest interactions leading to a ferro- or antiferro-magnetic exchange in the system is responsible for the magnetic frustration. Thence, the ANNNI model offers the possibility to study the competing mechanism of quantum fluctuations due to the transverse magnetic field and frustration. The phase diagram of the quantum model at $T = 0$ has been studied mainly by renormalization group or Montecarlo techniques in d dimensions exploiting also the correspondence with the classical analog in $d + 1$ dimensions [27–32]. The phase diagram is quite rich and three phases have been confirmed, separated by two second-order phase transitions. The first, for low frustration ($\kappa < 0.5$) of the Ising-type separates the ferromagnetic and the paramagnetic phases along the line $h_I(\kappa) \approx \frac{1-\kappa}{\kappa}\left(1 - \sqrt{\frac{1-3\kappa+4\kappa^2}{1-\kappa}}\right)$. The other one of

* oriel.kiss@cern.ch
† michele.grossi@cern.ch

a commensurate-incommensurate type appears between the paramagnetic phase and an antiphase for values of the field $h_C(\kappa) \approx 1.05\sqrt{(x-0.5)(x-0.1)}$, in the high frustration sector ($\kappa > 0.5$). As usual, the paramagnetic phase is the disordered one, in contrast with the two ordered phases: the ferromagnetic and the antiphase one. In particular, they are different because the former is characterized by all the spins aligned along the field direction, and the latter has a four-spin periodicity, composed of repetitions of two pairs of spins pointing in opposite directions. The point $\kappa = 0.5$ represents a multicritical point. We mention here that other relevant lines have been numerically addressed but not confirmed. One signaling an infinite-order phase transition of the Berezinskii–Kosterlitz–Thouless (BKT) type for $h_{BKT}(\kappa) \approx 1.05(\kappa - 0.5)$, delimiting a floating phase between the paramagnetic and the antiphase [31] and a disorder line where the model is exactly solvable known as the Peschel-Emery (PE) line $h_{PE}(\kappa) \approx \frac{1}{4\kappa} - \kappa$ [30, 33].

Variational State Preparation: The purpose of the Variational Quantum Eigensolver (VQE) [34] is to calculate the ground state energy of a Hamiltonian $H(\kappa, h)$ on a quantum computer. Using the Rayleigh-Ritz variational principle, the VQE minimizes the energy expectation value of a parametrized wavefunction and has been successfully applied in quantum chemistry [35–37], in nuclear physics [38–40] or in frustrated magnetic systems [41, 42]. Here, we are interested in the final eigenstates, represented by an ansatz $|\psi(\theta;\kappa,h)\rangle$, to be used as quantum data. Typically, the ansatz is chosen as an hardware-efficient quantum circuit [35, 43], which is built with low connectivity and gates that can be easily run on NISQ devices. For instance, we use $D = 6(9)$ repetitions of a layer consisting of free rotation around the y-axis $R_y(\theta) = e^{-i\theta\sigma_y/2}$ and CNOT gates with linear connectivity $\mathrm{CX}_{i,i+1}$ for $0 \leq i < N$ [44], where $H(\kappa, h)$ is the ANNNI model from Eq. 1 with $N = 6(12)$ spins.

Quantum Convolutional Neural Networks (QCNNs): QCNNs are a class of quantum circuits, inspired by classical convolutional neural networks (CNN), originally proposed in [21]. In our implementation, the QCNN starts with a free rotation layer around the y-axis, followed by blocks consisting of convolutions, free rotations, and pooling layers that halve the number of qubits to k until $k = \lceil \log_2(K) \rceil$, where K it the total number of quantum phases. Finally, a fully connected layer and measurement are performed in the computational basis. An example with $N = 6$ qubits is shown in Figure 1 where we have free y-axis rotations (yellow), $R(\vec{\theta}) = \bigotimes_{i=1}^{N} R_y(\vec{\theta}_i)$, two-qubit convolutions (light green) $C(\theta) = \bigotimes_{i=1}^{2} R_y(\theta)$, pooling (red) $P(\vec{\theta}, \phi, b) = R_y(\vec{\theta}_b)R_x(\phi)$ with $b \in \{0, 1\}$ the value of the measured qubit, and a two-qubit fully connected (dark green) gate

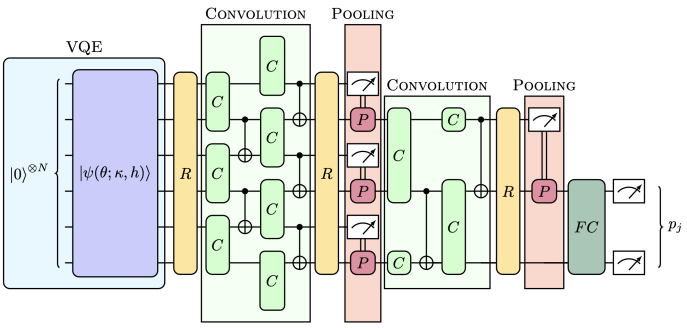

Figure 1: Circuit architecture: VQE states (blue) are the input of the Quantum Convolutional Neural Network composed of free rotations R (yellow), convolutions C (light green), pooling P (red) and a fully connected layer F (dark green).

$$F(\vec{\theta}^{(1)}, \vec{\theta}^{(2)}) = \left(\bigotimes_{i=1}^{2} R_y(\vec{\theta}_1^{(i)}) R_x(\vec{\theta}_2^{(i)}) R_y(\vec{\theta}_3^{(i)})\right) \mathrm{CX}_{1,2}.$$

QCNNs have been shown to be resistant to barren plateaus [45] due to their distance from low $T2$-design and are therefore good candidates for any quantum learning tasks. The analogy with CNN holds in the quantum settings since convolution and pooling layers are functions of shared parameters and the reduction of the circuit's dimension is guaranteed by the intermediate measurement. Even if mid-circuit measurements are currently not available on NISQ devices due to a time delay constraint between the classical and quantum hardware, a classical postprocessing step is nevertheless able to replicate their effect [24]. The whole algorithm flow starts with the QCNN taking as input ground states $|\psi(\theta;\kappa,h)\rangle$ from the Hamiltonian family $H(\kappa, h)$, obtained through the VQE. The quantum network then outputs the probability $p_j(\kappa, h)$ of being in one of the $K = 3$ phases (ferro-, para-magnetic or antiphase), where $p_j(\kappa, h)$ is computed as the probability of measuring the state $|01\rangle, |10\rangle, |11\rangle$ on the two output qubits. Since the phase diagram of the ANNNI model only contains three phases, the state $|00\rangle$ is interpreted as a *garbage* class.

The training data set consists of the composition of points from two analytical models derived from the simplification of the physical model used. Specifically, the integrable Ising model in transverse field in case $\kappa = 0$ and the *quasi*-classical model when $h = 0$, and there are no longer quantum fluctuations. We demonstrate that QCNNs extend its prediction to the all phase diagram when only trained on the marginal model given by $\mathcal{S}_X^n \subseteq \{(\kappa, h) \in \{0\} \times [0, 2]\} \cup \{(\kappa, h) \in [0, 1] \times \{0\}\}$. We consider two types of subsets $X \in \{G, N\}$, $\mathcal{S}_G^n$ where n training points are sampled normally around each critical point and $\mathcal{S}_U^n$ where n data points are drawn uniformly on both axes. In both cases, we have $|\mathcal{S}_n| = 2n$. The

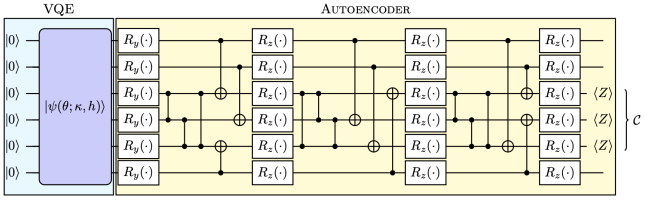

Figure 2: Compression circuit (yellow) and anomaly score measurement ($\mathcal{C}$) of the ground states of $H(\kappa, h)$ obtained through a VQE (blue). The $\cdot$ represent independent parameters.

QCNN is trained using the cross entropy $\mathcal{L}$ loss

$$\mathcal{L} = -\frac{1}{|\mathcal{S}_X^n|} \sum_{(\kappa,h)\in\mathcal{S}_X^n} \sum_{j=1}^{K} y_j(\kappa,h) \log\left(p_j(\kappa,h)\right) \quad (2)$$

between the one-hot classical labels $y_j(\kappa, h)$ and the predictions on the training region $\mathcal{S}_X^n$ of the phase space.

Anomaly Detection (AD): For the convenience of the reader, we will recall the unsupervised anomaly detection (AD) scheme, initially proposed by Kottmann *et al.* [25], to draw the phase diagram of the Bose-Hubbard model. Since it is an unsupervised learning technique, it bypasses the bottleneck of needing classical training labels and is, therefore, an alternative to the approach taken in this letter.

As a first step, an initial state $|\psi\rangle$ is chosen in the data set composed of the ground states of H. Although there is no formal restriction, it should lie far from any critical points. A quantum encoder [46] is then trained to learn to compress $|\psi\rangle$ on a $N > k$-qubit state $|\phi\rangle$ with quantum register q_C, i.e., to write $|\psi\rangle = |\phi\rangle \otimes |T\rangle$, where the latter is a $(N-k)$-qubit trash state with register q_T. In practice, an anomaly score based on the Hamming distance between the trash state $|T\rangle$ to $|0\rangle^{\otimes(N-k)}$, written as

$$\mathcal{C} = \frac{1}{2} \sum_{j\in q_T} (1 - \langle Z_j\rangle), \quad (3)$$

and we make the choice $k = N/2$. Intuitively, the encoder compresses similar states, i.e., states in the same phase, with success but will fail to compress states in a different phase, leading to a high anomaly score. The encoder, as proposed in [25], is composed of D layers of independent $R_y(\theta)$ rotations on all qubits and $\mathrm{CZ}_{i,j}$ gates for $i \in q_C, j \in q_T$ and $i, j \in q_T$ gates. We use a slightly modified version, with a first layer of $R_y(\cdot)$ individual rotations, followed by $D = 3$ layers composed of $\mathrm{CX}_{i,j}$ gates for $i \in q_C$ and $j \in q_T$, $\mathrm{CZ}_{i,j}$ gates with $i, j \in q_T$ and independent $R_z(\cdot)$ rotations as displayed in Figure 2 for $N = 6$.

We highlight a few differences with the supervised approach. First, the anomaly score measurement is highly dependent on the choice of the initial state $|\psi\rangle$, and can often lead to phase diagrams without any clear phase separation. Moreover, there is no quantitative way to assess the validity of the phase diagram, while with the QCNN we may evaluate the accuracy on the training set. Finally, the anomaly score only provided qualitative results. Hence, only a continuous number (the anomaly syndrome) is associated with each point, and there is no canonical way to assign it to a particular phase. On the other hand, the QCNN outputs the probability of being in each phase and therefore, the solution is to assign the most probable phase to it.

Results: At this point, once we have introduced the problem and defined the techniques used, we can analyze the quality of the results obtained under ideal conditions with a quantum simulator.

We study our ability to reconstruct the phase diagram of the ANNNI model, characterized by a non-trivial disordered paramagnetic phase, the ordered ferromagnetic and antiphase one. To test the stability of the proposed approach, we consider the model with an increasing number of spins $N = 6, 12$ and sampling a different number of points $0 < n \leq 100$ used for the training. By virtue of the quality of the results, we evaluated the influence of different sampling of the training points corresponding to the two physical models that could affect the quality of the classification. A summary of the results can be qualitatively seen in Figure 3. In the first row, we have the phase diagram reconstruction for the ANNNI model with 6 spins, where the white lines represent the analytical transition explained above in the model section. The second line in the figure shows the same for a system with $N = 12$ spins.

The first diagram shows the accuracy, computed on the whole phase space, as a function of the number of training points per axis n, for the Gaussian $X = G$ and uniform $X = U$ sampling scheme, where the error bars correspond to one standard deviation from ten independent runs. We observe that the accuracy quickly increases with n, before saturating for $n \geq 14$, as argued in Ref. [26]. The second plot is the phase diagram obtained with training on $n = 14$ points, where this number represents the minimum number of points able to reach the maximum accuracy. The third plot instead is the comparison to the unsupervised learning approach inspired from [25] where the autoencoder is trained on the single red cross $|\psi\rangle$. It is worth noting that although only one point is sufficient to obtain a qualitatively good phase diagram, only the approach proposed in this work with QCNNs allows a quantitative prediction for the phase. In terms of accuracy of the data points, the error as a difference between the VQE outcome and the numerical solution is on average below 1% on the transition zones while there is almost no error elsewhere. Colour shades represent the continuous probability distribution of the QCNN for our multiclass classifier as a probability mixture, where spare points are given by

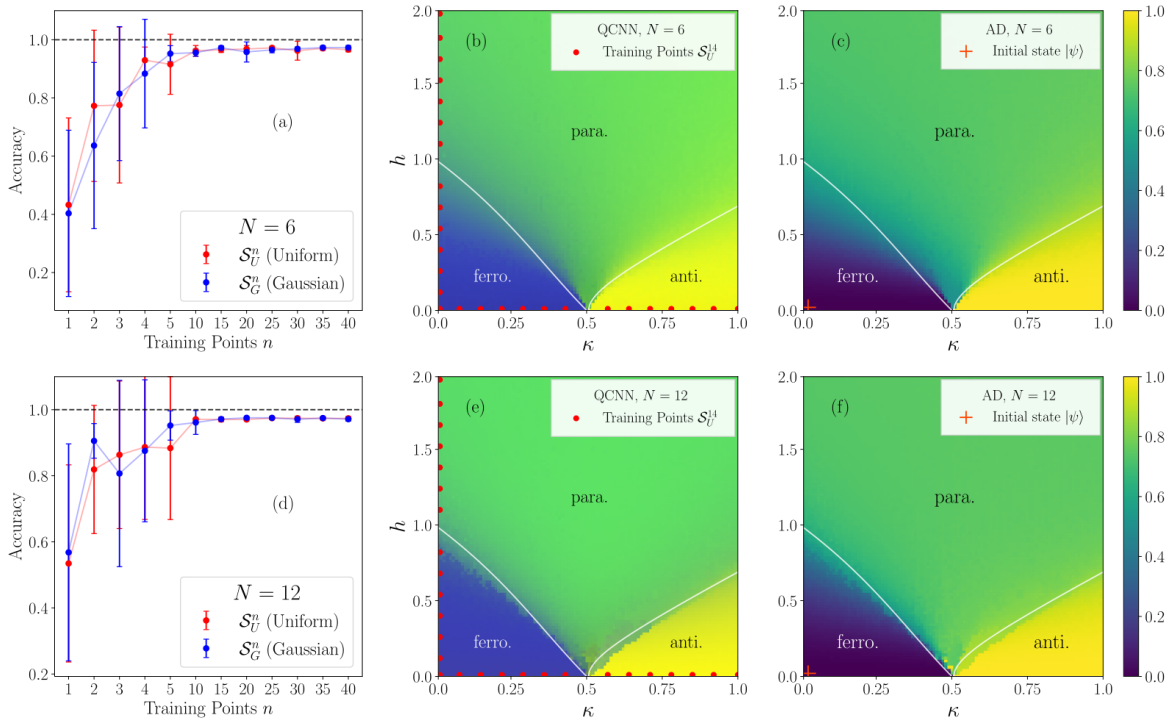

Figure 3: Quantum Phases Classification. Panel (a) shows the classification accuracy of the QCNN as a function of the number of training points per axis n, for the Gaussian (blue) and Uniform sampling (red), (b) displays the phase diagram predicted by the QCNN trained on $\mathcal{S}_U^{14}$ (red dots) where the color represents the probability mixture of being in one of the three phases, while (c) shows the anomaly score for a $N = 6$ spins systems trained on the initial state $|\psi\rangle$ (red cross). The panels (d), (e) and (f) are similar but for $N = 12$ spins. The solid white lines are $h_I(\kappa)$ for $\kappa < 0.5$ and $h_C(\kappa)$ for $\kappa > 0.5$

quantum fluctuations.

Conclusion: This letter addresses the computation of the phase diagram of a non-integrable model, by training a QCNN on the limiting integrable regions of the considered ANNNI model. The numerical simulations suggest that QCNNs can carry this task with more than 95% accuracy, using only $2n = 28$ quantum data points on the two axes of the phase space. The accuracy of the QCNN quickly increases to reach its maximum as a function of the number of training points, suggesting that QCNNs can generalise from a few data points. Moreover, the performance of the algorithm seems to improve with the system's size. Hence, the training loss is smaller for $N = 12$ than for $N = 6$ and the predicted boundaries in the phase space are also clearer, meaning that the QCNN is more confident. Even if this could be caused by the reduction of boundary or finite-size effects, it hints towards scalability of the proposed model, provided the availability of quantum data. However, being a supervised method, the QCNN is not able to detect phases that are not present in the training set $\mathcal{S}_X^n$, i.e., the boundaries, such as the BKT phase transition and the PE line. Future work should be performed in this direction, by either affording $\mathcal{O}(1)$ training points inside these unrepresented phases or mixing the QCNN with the unsupervised approach.

ACKNOWLEDGMENTS

SM, OK, SV and MG are supported by CERN Quantum Technology Initiative. AM is supported by Foundation for Polish Science (FNP), IRAP project ICTQT, contract no. 2018/MAB/5, co-financed by EU Smart Growth Operational Program, and (Polish) National Science Center (NCN), MINIATURA DEC-2020/04/X/ST2/01794.

[1] Jacob Biamonte, Peter Wittek, Nicola Pancotti, Patrick Rebentrost, Nathan Wiebe, and Seth Lloyd, "Quantum machine learning," Nature **549**, 195–202 (2017).

[2] Marcello Benedetti, Erika Lloyd, Stefan Sack, and Mattia Fiorentini, "Parameterized quantum circuits as machine learning models," Quantum Science and Technology **4**, 4 (2019).

[3] Oriel Kiss, Francesco Tacchino, Sofia Vallecorsa, and Ivano Tavernelli, "Quantum neural networks force field generation," Mach. Learn.: Sci. Technol. **3** (2022), https://doi.org/10.1088/2632-2153/ac7d3c.

[4] Vishal S. Ngairangbam, Michael Spannowsky, and Michihisa Takeuchi, "Anomaly detection in high-energy physics using a quantum autoencoder," Phys. Rev. D **105**, 095004 (2022).

[5] Chen Zhou, Jay Chan, Wen Guan, Shaojun Sun, Alex Zeng Wang, Sau Lan Wu, Miron Livny, Federico Carminati, Alberto Di Meglio, Andy C. Y. Li, Joseph Lykken, Panagiotis Spentzouris, Samuel Yen-Chi Chen, Shinjae Yoo, and Tzu-Chieh Wei, "Application of Quantum Machine Learning to High Energy Physics Analysis at LHC using IBM Quantum Computer Simulators and IBM Quantum Computer Hardware," PoS **ICHEP2020**, 930 (2021).

[6] Sau Lan Wu, Jay Chan, Wen Guan, Shaojun Sun, Alex Wang, Chen Zhou, Miron Livny, Federico Carminati, Alberto Di Meglio, Andy C Y Li, Joseph Lykken, Panagiotis Spentzouris, Samuel Yen-Chi Chen, Shinjae Yoo, and Tzu-Chieh Wei, "Application of quantum machine learning using the quantum variational classifier method to high energy physics analysis at the LHC on IBM quantum computer simulator and hardware with 10 qubits," Journal of Physics G: Nuclear and Particle Physics **48**, 125003 (2021).

[7] YaoChong Li, Ri-Gui Zhou, RuQing Xu, Jia Luo, and WenWen Hu, "A quantum deep convolutional neural network for image recognition," Quantum Science and Technology **5**, 044003 (2020).

[8] K. Mitarai, M. Negoro, M. Kitagawa, and K. Fujii, "Quantum circuit learning," Phys. Rev. A **98**, 032309 (2018).

[9] Daniel Mills Brian Coyle, Vincent Danos, and Elham Kashefi, "The born supremacy: quantum advantage and training of an ising born machine," npj Quantum Inf **6**, 60 (2020).

[10] Christa Zoufal, Aurélien Lucchi, and Stefan Woerner, "Quantum generative adversarial networks for learning and loading random distributions," npj Quantum Inf **5** (2019), https://doi.org/10.1038/s41534-019-0223-2.

[11] Manuel S. Rudolph, Ntwali Bashige Toussaint, Amara Katabarwa, Sonika Johri, Borja Peropadre, and Alejandro Perdomo-Ortiz, "Generation of high-resolution handwritten digits with an ion-trap quantum computer," Phys. Rev. X **12**, 031010 (2022).

[12] Oriel Kiss, Michele Grossi, Enrique Kajomovitz, and Sofia Vallecorsa, "Conditional born machine for monte carlo events generation," ArXiv e-prints (2022), arXiv:2205.07674 [quant-ph].

[13] Andrea Delgado and Kathleen E. Hamilton, "Unsupervised quantum circuit learning in high energy physics," ArXiv e-prints (2022), arXiv:2203.03578 [quant-ph].

[14] Amira Abbas, David Sutter, Christa Zoufal, Aurelien Lucchi, Alessio Figalli, and Stefan Woerner, "The power of quantum neural networks," Nature Computational Science **1**, 403–409 (2021).

[15] Hsin-Yuan Huang, Michael Broughton, Masoud Mohseni, Ryan Babbush, Sergio Boixo, Hartmut Neven, and Jarrod R. McClean, "Power of data in quantum machine learning," Nat Commun **2631** (2021), https://doi.org/10.1038/s41467-021-22539-9.

[16] Jennifer R. Glick, Tanvi P. Gujarati, Antonio D. Corcoles, Youngseok Kim, Abhinav Kandala, Jay M. Gambetta, and Kristan Temme, "Covariant quantum kernels for data with group structure," ArXiv e-prints (2021), arXiv:2105.03406 [quant-ph].

[17] Maria Schuld and Nathan Killoran, "Is quantum advantage the right goal for quantum machine learning?" PRX Quantum **3**, 030101 (2022).

[18] Rishi Bommasani *et al.*, "On the opportunities and risks of foundation models," (2022), arXiv:2108.07258 [cs.LG].

[19] Hsin-Yuan Huang, Michael Broughton, Jordan Cotler, Sitan Chen, Jerry Li, Masoud Mohseni, Hartmut Neven, Ryan Babbush, Richard Kueng, John Preskill, and Jarrod R. McClean, "Quantum advantage in learning from experiments," Science **376**, 1182–1186 (2022).

[20] Christian D. Marciniak, Thomas Feldker, Ivan Pogorelov, Raphael Kaubruegger, Denis V. Vasilyev, Rick van Bijnen, Philipp Schindler, Peter Zoller, Rainer Blatt, and Thomas Monz, "Optimal metrology with programmable quantum sensors," Nature **603**, 604–609 (2022).

[21] Iris Cong, Soonwon Choi, and Mikhail D. Lukin, "Quantum convolutional neural networks," Nat. Phys. **15**, 1273–1278 (2019).

[22] A. V. Uvarov, A. S. Kardashin, and J. D. Biamonte, "Machine learning phase transitions with a quantum processor," Phys. Rev. A **102**, 012415 (2020).

[23] Marco Lazzarin, Davide Emilio Galli, and Enrico Prati, "Multi-class quantum classifiers with tensor network circuits for quantum phase recognition," Physics Letters A **434**, 128056 (2022).

[24] Johannes Herrmann, Sergi Masot Llima, Ants Remm, Petr Zapletal, Nathan A. McMahon, Colin Scarato, François Swiadek, Christian Kraglund Andersen, Christoph Hellings, Sebastian Krinner, Nathan Lacroix, Stefania Lazar, Michael Kerschbaum, Dante Colao Zanuz, Graham J. Norris, Michael J. Hartmann, Andreas Wallraff, and Christopher Eichler, "Realizing quantum convolutional neural networks on a superconducting quantum processor to recognize quantum phases," Nat Commun **13** (2022), https://doi.org/10.1038/s41467-022-31679-5.

[25] Korbinian Kottmann, Friederike Metz, Joana Fraxanet, and Niccolò Baldelli, "Variational quantum anomaly detection: Unsupervised mapping of phase diagrams on a physical quantum computer," Phys. Rev. Research **3**, 043184 (2021).

[26] Matthias C. Caro, Hsin-Yuan Huang, M. Cerezo, Kunal Sharma, Andrew Sornborger, Lukasz Cincio, and Patrick J. Coles, "Generalization in quantum machine learning from few training data," ArXiv e-prints (2021), arXiv:2111.05292 [quant-ph].

[27] Walter Selke, "The annni model — theoretical analysis and experimental application," Physics Reports **170**, 213–264 (1988).

[28] Paulo R. Colares Guimarães, João A. Plascak, Francisco C. Sá Barreto, and João Florencio, "Quantum phase transitions in the one-dimensional transverse ising model with second-neighbor interactions," Phys. Rev. B **66**, 064413 (2002).

[29] Anjan Kumar Chandra and Subinay Dasgupta, "Floating phase in the one-dimensional transverse axial next-

nearest-neighbor ising model," Phys. Rev. E **75**, 021105 (2007).
[30] Matteo Beccaria, Massimo Campostrini, and Alessandra Feo, "Density-matrix renormalization-group study of the disorder line in the quantum axial next-nearest-neighbor ising model," Phys. Rev. B **73**, 052402 (2006).
[31] Matteo Beccaria, Massimo Campostrini, and Alessandra Feo, "Evidence for a floating phase of the transverse annni model at high frustration," Phys. Rev. B **76**, 094410 (2007).
[32] Askery Canabarro, Felipe Fernandes Fanchini, André Luiz Malvezzi, Rodrigo Pereira, and Rafael Chaves, "Unveiling phase transitions with machine learning," Phys. Rev. B **100**, 045129 (2019).
[33] I Peschel and VJ Emery, "Calculation of spin correlations in two-dimensional ising systems from one-dimensional kinetic models," Zeitschrift für Physik B Condensed Matter **43**, 241–249 (1981).
[34] Alberto Peruzzo, Jarrod McClean, Peter Shadbolt, Man-Hong Yung, Xiao-Qi Zhou, Peter J. Love, Alán Aspuru-Guzik, and Jeremy L. O'Brien, "A variational eigenvalue solver on a photonic quantum processor," Nature Communications **5**, 4123 (2014).
[35] Abhinav Kandala, Antonio Mezzacapo, Kristan Temme, Maika Takita, Markus Brink, Jerry M. Chow, and Jay M. Gambetta, "Hardware-efficient variational quantum eigensolver for small molecules and quantum magnets," Nature **549**, 242–246 (2017).
[36] Panagiotis Kl. Barkoutsos, Jerome F. Gonthier, Igor Sokolov, Nikolaj Moll, Gian Salis, Andreas Fuhrer, Marc Ganzhorn, Daniel J. Egger, Matthias Troyer, Antonio Mezzacapo, Stefan Filipp, and Ivano Tavernelli, "Quantum algorithms for electronic structure calculations: Particle-hole hamiltonian and optimized wavefunction expansions," Phys. Rev. A **98**, 022322 (2018).
[37] Jonathan Romero, Ryan Babbush, Jarrod R McClean, Cornelius Hempel, Peter J Love, and Alán Aspuru-Guzik, "Strategies for quantum computing molecular energies using the unitary coupled cluster ansatz," Quantum Sci. Technol. **4**, 014008 (2019).
[38] E. F. Dumitrescu, A. J. McCaskey, G. Hagen, G. R. Jansen, T. D. Morris, T. Papenbrock, R. C. Pooser, D. J. Dean, and P. Lougovski, "Cloud quantum computing of an atomic nucleus," Phys. Rev. Lett. **120**, 210501 (2018).
[39] I. Stetcu, A. Baroni, and J. Carlson, "Variational approaches to constructing the many-body nuclear ground state for quantum computing," Phys. Rev. C **105**, 064308 (2022).
[40] Oriel Kiss, Michele Grossi, Pavel Lougovski, Federico Sanchez, Sofia Vallecorsa, and Thomas Papenbrock, "Quantum computing of the ^{6}li nucleus via ordered unitary coupled cluster," ArXiv e-prints (2022), arXiv:2205.00864 [nucl-th].
[41] Alexey Uvarov, Jacob D. Biamonte, and Dmitry Yudin, "Variational quantum eigensolver for frustrated quantum systems," Phys. Rev. B **102**, 075104 (2020).
[42] Michele Grossi, Oriel Kiss, Francesco De Luca, Carlo Zollo, Ian Gremese, and Antonio Mandarino, "Finite-size criticality in fully connected spin models on superconducting quantum hardware," ArXiv e-prints (2022), arXiv:2208.02731 [quant-ph].
[43] Sukin Sim, Peter D. Johnson, and Alán Aspuru-Guzik, "Expressibility and entangling capability of parameterized quantum circuits for hybrid quantum-classical algorithms," Advanced Quantum Technologies **2**, 1900070 (2019).
[44] Michael A. Nielsen and Isaac L. Chuang, *Quantum Computation and Quantum Information: 10th Anniversary Edition* (Cambridge University Press, 2010).
[45] Arthur Pesah, M. Cerezo, Samson Wang, Tyler Volkoff, Andrew T. Sornborger, and Patrick J. Coles, "Absence of barren plateaus in quantum convolutional neural networks," Phys. Rev. X **11**, 041011 (2021).
[46] Jonathan Romero, Jonathan P Olson, and Alan Aspuru-Guzik, "Quantum autoencoders for efficient compression of quantum data," Quantum Science and Technology **2**, 045001 (2017).